
EFDA–JET–CP(01)02-86

D. Testa, A. Fasoli, A. Jaun, T. Bolzonella, C. Challis,
J. Mailloux, F. Milani, P. de Vries
and JET EFDA Contributors

Measurement of the Damping Rate of Stable AEs on the JET Tokamak in Limiter and Diverted Plasmas with Monotonic and Non Monotonic q -Profiles

Measurement of the Damping Rate of Stable AEs on the JET Tokamak in Limiter and Diverted Plasmas with Monotonic and Non Monotonic q-Profiles

D. Testa¹, A. Fasoli¹, A. Jaun², T. Bolzonella³, C. Challis⁴,
J. Mailloux⁴, F. Milani⁴, P. de Vries⁵
and JET EFDA Contributors*

¹*Plasma Science and Fusion Center, Massachusetts Institute of Technology, Boston, USA.*

²*Euratom — Alfvén Laboratory, Royal Institute of Technology, Stockholm, Sweden.*

³*Consorzio RFX, Associazione Euratom-Eneasulla Fusione, 35127 Padova, Italy.*

⁴*Euratom — UKAEA Fusion Association, Culham Science Center, Abingdon, UK.*

⁵*Association EURATOM FOM – Rijnhuizen, TEC, PO Box 1207, 3430 BE Nieuwegein, NL*

**See appendix of the paper by J.Pamela “Overview of recent JET results”,*

Proceedings of the IAEA conference on Fusion Energy, Sorrento 2000

“This document is intended for publication in the open literature. It is made available on the understanding that it may not be further circulated and extracts or references may not be published prior to publication of the original when applicable, or without the consent of the Publications Officer, EFDA, Culham Science Centre, Abingdon, Oxon, OX14 3DB, UK.”

“Enquiries about Copyright and reproduction should be addressed to the Publications Officer, EFDA, Culham Science Centre, Abingdon, Oxon, OX14 3DB, UK.”

ABSTRACT

Systematic measurements of the frequency and damping rate of stable $n=0-2$ modes in the Alfvén frequency range are obtained on the JET tokamak in various plasma operating regimes. The JET saddle coils are used as external antennas to drive and detect stable AEs. The diagnostic technique uses repetitive sweeps of the driving frequency in a pre-defined range [1,2], controlled in real-time. The plasma response is extracted from background noise using synchronous detection, and is used to identify in real-time the resonance corresponding to a global mode. When a resonance is found, the real-time controller locks to that frequency and tracks the mode.

1. DAMPING RATE OF AES IN THE CONVENTIONAL TOKAMAK SCENARIO

The dependence of the measured damping rate upon the bulk plasma beta, the magnetic shear and the normalized Larmor radius has been analyzed in the conventional tokamak scenario, with monotonic q-profile. This study aims at discriminating between the different models for the AE damping mechanisms, to provide accurate extrapolation for burning fusion plasma experiments.

Figure 1 [2] shows the measured damping rate for $n=0$ Global AEs (GAEs) and $n=1$ Toroidal AEs (TAEs) as a function of the triangularity $\langle\delta\rangle=(\delta_{UP}+\delta_{LOW})/2$ averaged above and below the plasma midplane and the elongation at mid radius $\kappa(r/a=0.5)=\kappa_0+(\kappa_{95}-\kappa_0)(r/a)2/(0.95)2$. In this regime it is found that the high edge shear strongly stabilizes the low- n AEs, not the Xpoint itself. This result agrees with the theoretical predictions of the PENN code [3].

This extreme sensitivity of the AE damping rate upon the edge shape parameters may lead to a method to control in real-time the stability of fast ions resonating with AE global wave fields [2]. Figure 2 shows the measured γ/ω for a $n=1$ TAE in a discharge where PNBI was ramped-up to study the effect of T_i and β : γ/ω is predicted to increase with β for high- n AEs [4]. It is found that the increase in β causes a frequency splitting in the mode structure, contributing to reducing γ/ω , up to $P_{NBI}\approx 5\text{MW}$. Two other modes are measured during the same frequency scan, for $14<t(\text{s})<15$, at $P_{NBI}>2\text{MW}$, with $\gamma/\omega<0.5\%$. This result is consistent with the theoretical prediction of splitting of a single TAE into multiple kinetic AEs [5].

Another example of frequency splitting during the NBI phase is shown in Fig.3, where a single $n=1$ TAE (ohmic phase) splits into two $n=1$ AEs at $P_{NBI}=3\text{MW}$ with $|f_1-f_2|/f\approx 2.5\%$.

Conversely, Fig.4 shows that, for a similar background plasma, at higher $P_{NBI}>7\text{MW}$ the $n=1$ TAE being tracked is lost. A different $n=1$ mode is then detected at $t=13.6\text{s}$ and $t=14\text{s}$ with $f\approx 140\text{kHz}$ and $\gamma/\omega\approx 3.5\%$ at higher $P_{NBI}\approx 7-10\text{MW}$. In other discharges, $n=0-2$ AEs are observed at a different frequency, higher than that of the mode that was tracked, and with even larger γ/ω .

Between the various mechanisms that have been proposed to account for the AE damping rate, the so-called “radiative damping” [6] shows a clear dependence on the ion Larmor radius ρ_* and the λ -parameter, $\lambda=nq\rho_*(R/r)^{3/2}$. Figure 5 shows the variation of γ/ω for a $n=1$ TAE as function of ρ_* and λ during a discharge where the magnetic field and plasma current were ramped at fixed q_0 and q_{95} to change ρ_* , and hence λ , without significantly affecting the background plasma. We notice that the measured γ/ω is independent of ρ_* and λ .

2. DAMPING RATE OF AES IN THE ADVANCED TOKAMAK SCENARIO

A new line of experiments has focused on the role of the high central safety factor, $q_0 > 5$, in the advanced tokamak regimes, such as the JET Optimized Shear experiments with a non-monotonic q -profile in the presence of internal transport barriers, where the ion diamagnetic drift frequency approaches the AE frequency, $\omega_{*i}/\omega_{*i} > 0.1$. Coupling between drift- and kinetic-Alfvén waves is expected for $\omega_{*i}/\omega_{TAE} \approx 2nq^2 \rho_*^2 (R\omega_{pi}/c) > 0.01n$ [7], which could give rise to drift-kinetic AEs [7]. For the first time, and contrary to the conventional tokamak scenario, weakly damped low- n Alfvénic modes have been detected in diverted plasmas with very high edge magnetic shear, thus indicating a potential danger for alpha-driven AEs in reactor relevant regimes. Figure 6 shows an example of such measurements. Multiple $n=0-2$ resonances are observed in the AE frequency range: the weakly damped modes at $f/f_{TAE} \approx 0.4 \div 0.6$ do not follow the simple f_{TAE} frequency.

SUMMARY AND CONCLUSIONS.

In the conventional tokamak scenario, the linear stability of low- n AEs has been studied as a function of the plasma shape, ρ_* and β . It is found that γ/ω is very sensitive to the edge shaping (κ , δ), which suggests a real-time control mechanism for AEs approaching the marginal stability limit. The predictions of an increase in the AE damping rate with β for intermediate and high- n AEs are now being challenged by the data for low- n AEs, which show a reduction in γ/ω for increasing β and a splitting in the mode structure that may be accounted for through excitation of kinetic AEs. Finally, the measured γ/ω is independent of ρ_* and λ , which is inconsistent with the radiative damping model. For the advanced tokamak scenarios, weakly damped modes have been detected in the Alfvén frequency range: these modes are unaffected by the edge shear, contrary to the conventional tokamak scenario.

ACKNOWLEDGEMENTS

This work has been conducted under the European Fusion Development Agreement. D. Testa and A. Fasoli were partly supported by DoE contract No. DE-FG02-99ER54563.

REFERENCES

- [1]. A. Fasoli et al., *Phys. Rev. Lett.* **75**, 645 (1995); A. Fasoli et al., *Phys. Plasmas* **7**, 1816 (2000).
- [2]. D. Testa and A. Fasoli, *Nucl. Fusion* **41** (2001), *in press*.
- [3]. A. Jaun, A. Fasoli and D. Testa, *Phys. Lett.* **A265**, 288 (2000).
- [4]. A. Jaun et al., *Nucl. Fusion* **39**, 2095 (1999).
- [5]. A. Jaun et al., *Plasma Phys. Control. Fusion* **39**, 549 (1997).
- [6]. G.Y. Fu et al., *Phys Plasmas* **3**, 4036 (1996). [7] A. Jaun et al., *Nucl. Fusion* **40**, 1343 (2000).

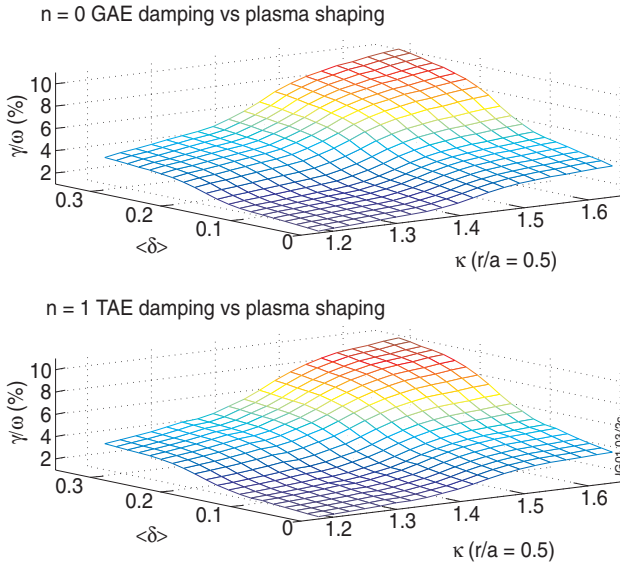


Figure 1: [2] shows the measured damping rate for $n=0$ Global AEs (GAEs) and $n=1$ Toroidal AEs (TAEs) as a function of the triangularity $\langle \delta \rangle = (\delta_{UP} + \delta_{LOW})/2$ averaged above and below the plasma midplane and the elongation at mid radius $\kappa(r/a=0.5) = \kappa_0 + (\kappa_{95} - \kappa_0)(r/a)^2 / (0.95)^2$.

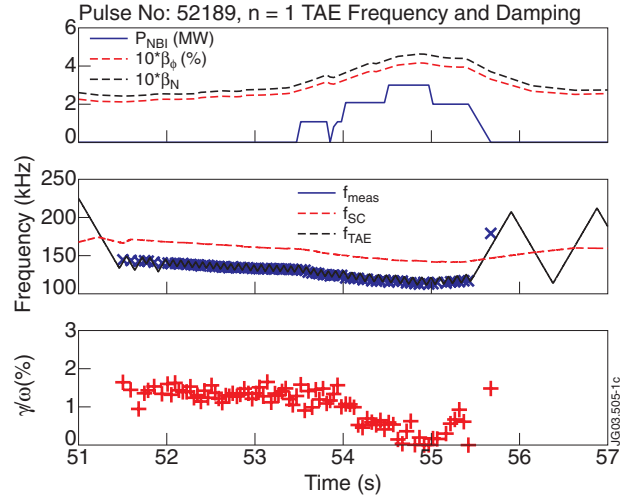


Figure 2: Plasma in limiter configuration with $q_0 \approx 0.9$, $q_{95} \approx 3.2$, $\sigma_0 \approx 1.1$, $\sigma_{95} \approx 9.5$, $\kappa_0 \approx 1.2$, $\kappa_{95} \approx 1.4$, $\delta_{UP} \approx 0.05$, $\delta_{LOW} \approx 0.07$, $n_{e0} \approx 2.5 \times 10^{19} m^{-3}$, $T_{e0} \approx 2.5 keV$.

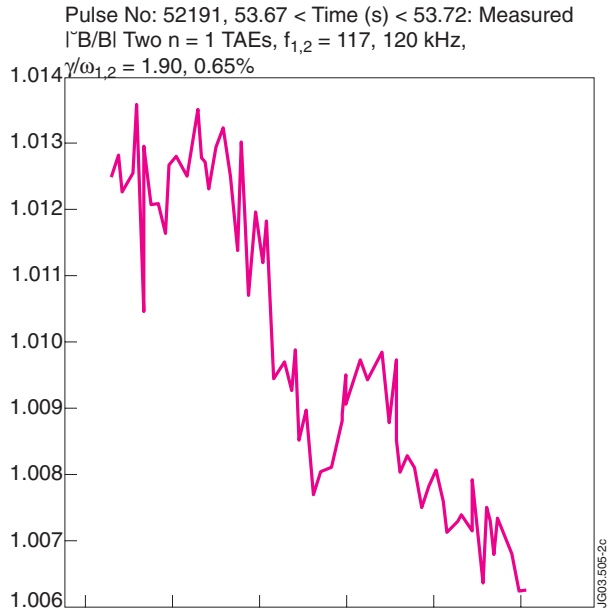
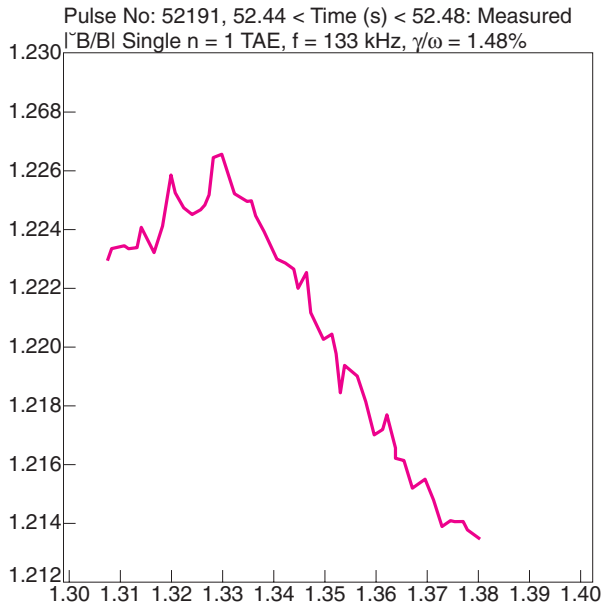


Figure 3: Left: ohmic phase, right: $P_{NBI} = 3MW$. During this entire phase the main plasma parameters are $q_0 \approx 0.8$, $q_{95} \approx 3.2$, $\sigma_0 \approx 1.1$, $\sigma_{95} \approx 9.8$, $\kappa_0 \approx 1.2$, $\kappa_{95} \approx 1.4$, $\delta_{UP} \approx 0.06$, $\delta_{LOW} \approx 0.08$, $n_{e0} \approx 2.2 \rightarrow 3.2 \times 10^{19} m^{-3}$, $T_{i0} \approx 1.5 keV$ and $T_{e0} \approx 3 keV$.

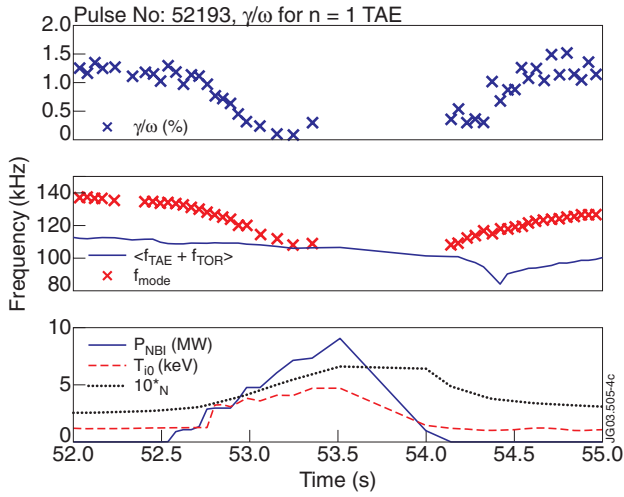


Figure 4: Shows that, for a similar background plasma, at higher $P_{NBI} > 7\text{MW}$ the $n=1$ TAE being tracked is lost.

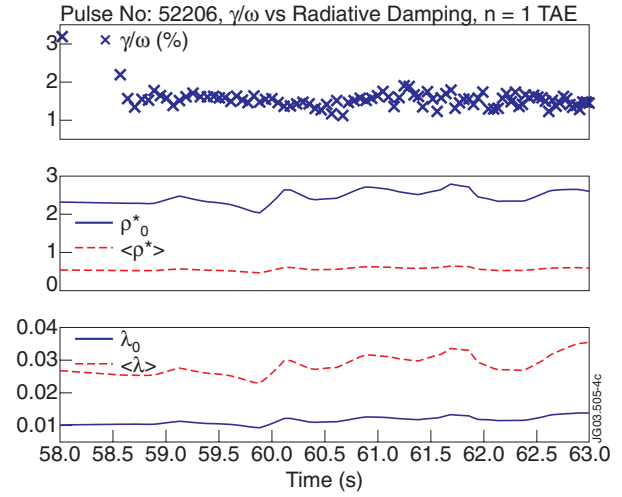


Figure 5: Plasma in limiter configuration with $q_0 \approx 0.9$, $q_{95} \approx 3$, $\sigma_0 \approx 1$, $\sigma_{95} \approx 9.2$, $\kappa_0 \approx 1.2$, $\kappa_{95} \approx 1.35$, $\delta_{UP} \approx 0.04$, $\delta_{LOW} \approx 0.07$, $T_{e0} \approx 1.5\text{keV}$, $\langle T_e \rangle \approx 1\text{keV}$, $n_{e0} \approx 1.7 \times 10^{19}\text{m}^{-3}$.

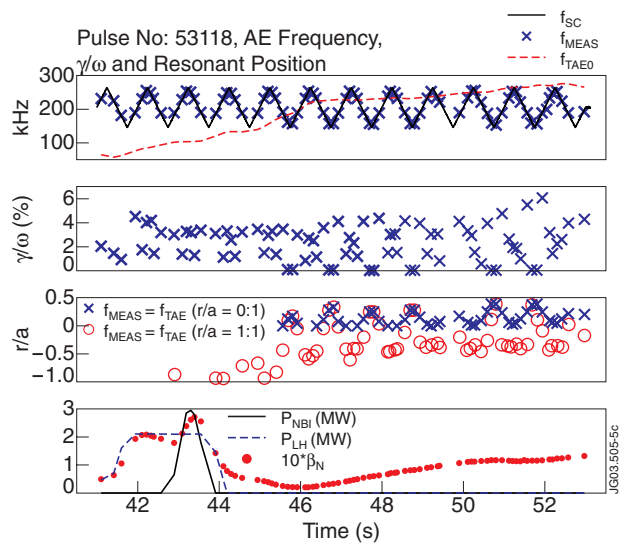
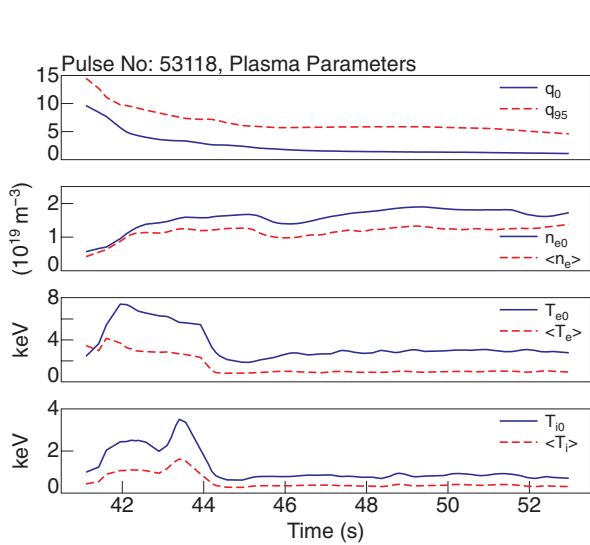


Figure 6: Plasma in X-point configuration: $\kappa_0 \approx 1.5 \rightarrow 1.3$, $\kappa_{95} \approx 1.7 \rightarrow 1.6$, $\delta_{UP} \approx 0.13 \pm 0.21$, $\delta_{LOW} \approx 0.17 \pm 0.25$. Modes at $f_{MEAS} \approx f_{TAE0}$ have $\gamma/\omega \approx 3-6\%$; modes at $f_{MEAS} \approx 0.7 f_{TAE0}$ have $\gamma/\omega \approx 1-2\%$; modes at $f_{MEAS} \approx 0.5 f_{TAE0}$ have $\gamma/\omega < 0.5\%$.